Deep Mining 2024 – P Andrieux & D Cumming-Potvin (eds)
© 2024 Australian Centre for Geomechanics, Perth, ISBN 978-0-6450938-9-6
doi:10.36487/ACG_repo/2465_42

Forecasting shaking and bulking ground velocities around tunnels for a planned mining sequence

Dmitriy Malovichko [a,*], Alex Rigby [a], Kashi Jessu [b], Gisela Viegas [b]

[a] *Institute of Mine Seismology, Australia*

[b] *Newmont Corporation, Australia*

Abstract

The assessment of expected ground velocities at the perimeter of tunnels is important for the quantification of dynamic demand imposed on ground support. Two types of ground velocities need to be considered. The first is the velocity of ground motion/shaking due to a stress wave from a remote (relative to the tunnel) seismic event, which is used to assess the likelihood of shakedown damage. The second is the velocity of bulking due to sudden stress fracturing on the perimeter of tunnel, which is used in the assessment of the likelihood of strainburst damage. We demonstrate procedures for forecasting both velocities using an example of a planned mining sequence at an Australian hard rock underground mine

Keywords: *seismic shakedown, strainbursting, ground support*

1 Introduction

The two rockburst damage mechanisms shown in Figure 1 require consideration of different types of ground velocities when evaluating the dynamic demand imposed on the ground support installed in a tunnel:

- Velocity of ground motion/shaking due a stress wave from a remote (relative to the tunnel) seismic event. Typically the peak value in the time history of shaking is identified (peak ground velocity, PGV) and used in the quantification of demand. Note that the velocity of motion of a supported block of ground can be different from the PGV. This difference depends on the block's mass, parameters of ground support and the frequency content of ground shaking as discussed by Malovichko & Kaiser (2020).
- Velocity of bulking (or strainbursting) due to sudden stress fracturing on the tunnel's perimeter, i.e. the velocity at which the volume of stress-fractured rock moves into the excavation.

It is important to keep in mind that a strainburst produces ground motion in the surrounding rock mass. The radiated seismic waves can be recorded by a seismic monitoring system and classified as a seismic event. However, this shaking is not the cause of strainburst damage: it is a byproduct of it. Correspondingly, the near-source PGV evaluated from recorded seismic signals cannot be used to assess the dynamic demand imposed on ground support within the bursting volume. The velocity of bulking must be used instead. This aspect is illustrated in Figure 2, which shows the evolution of a strainburst around a circular tunnel as modelled by Rigby et al. (2024).

* Corresponding author. Email address: dmitriy.malovichko@imsi.org

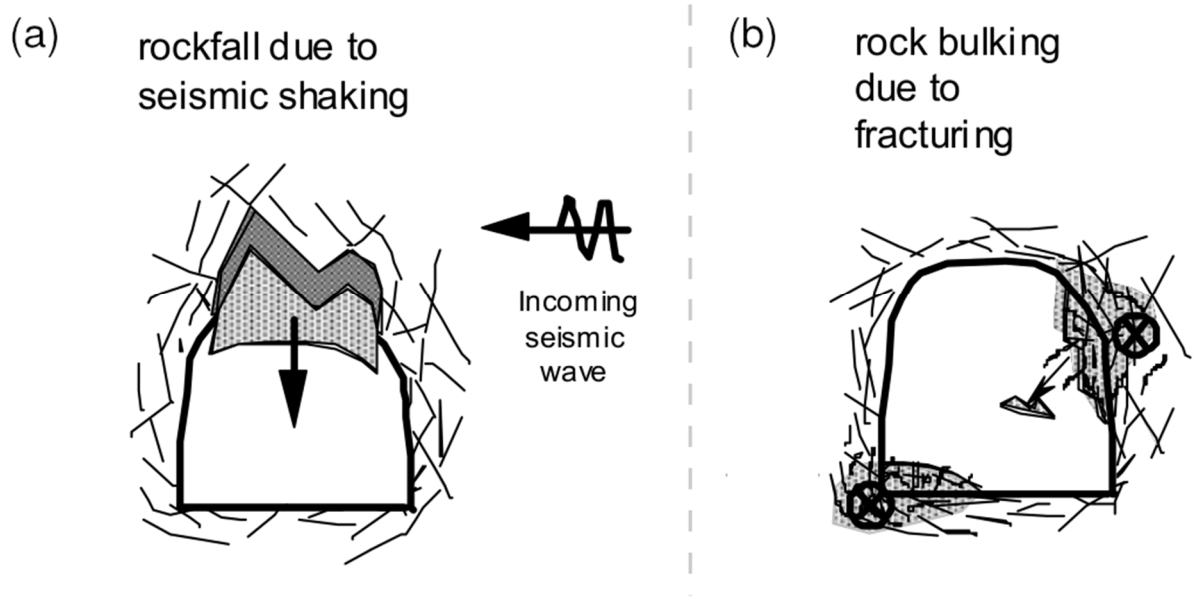

Figure 1 **Two types of rockbursts described in Kaiser & Moss (2022) based on Kaiser et al. (1996): (a) Shakedown, which causes damage to an excavation or its support by a seismically induced fall of ground; (b) Strainburst, which is an excavation or support failure process whereby a highly stressed volume of unsupported or supported rock bursts near an excavation**

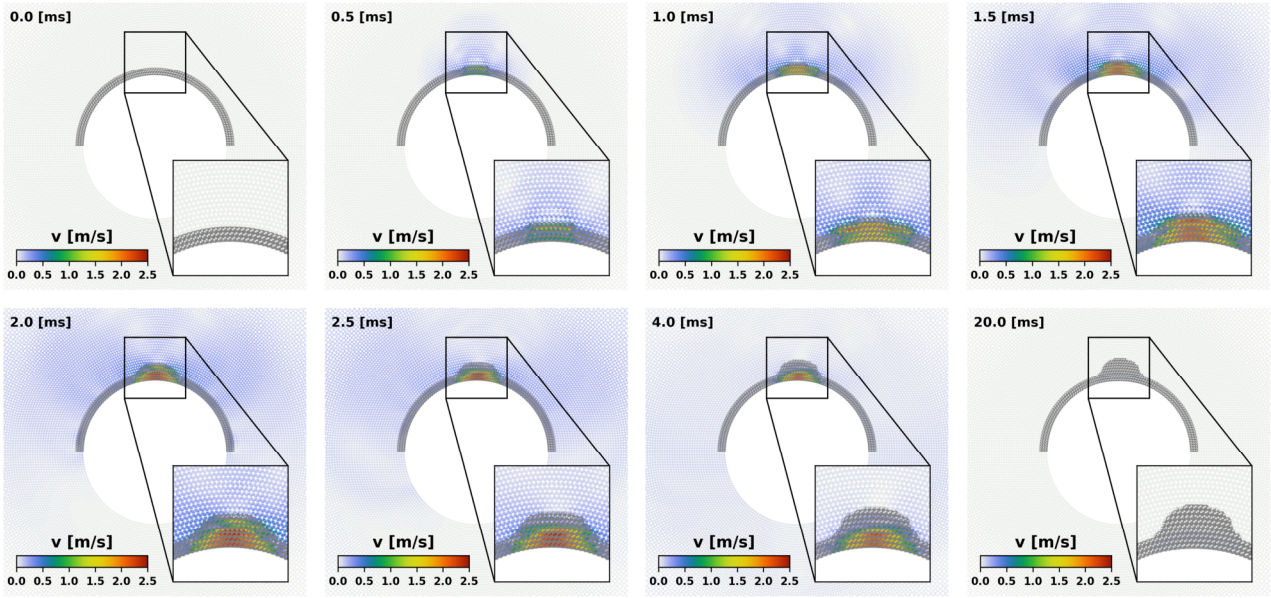

Figure 2 **2D modelling of dynamic stress fracturing on the perimeter of a cylindrical tunnel loaded by horizontal maximum principal stress (Rigby et al. 2024). Grey area describes damaged rock. The failure nucleates spontaneously above the pre-existing damage zone at time 0 ms. The failure evolves dynamically, radiating seismic waves. Finally, at time 20 ms, the rock mass around the tunnel settles into a stable state**

The maximum velocity of ground motion generated around the tunnel during dynamic stress fracturing in the modelled example is 0.25 m/s, while the maximum velocity of ground within the fracturing volume is of the order of magnitude higher, approaching 2.5 m/s. The latter can be evaluated from the following measurable parameters (Kaiser & Moss 2022):

- the increase in the depth of damage (or depth of strainbursting), d_{SB}, which is approximately 0.5 m in the shown case (see the difference in grey areas between the first and last image in Figure 2)
- the duration of stress fracturing and the convergence of rock mass surrounding the tunnel, t_{SB}, which is approximately 15 ms in the example presented
- the bulking factor (BF) which can be taken as between 2 and 4% in the considered example.

The resulting estimate of average bulking/strainbursting velocity, $V_{SB} = (BF/100) \cdot d_{SB}/t_{SB}$, is 0.7–1.3 m/s, is consistent with the maximum modelled velocity quoted above.

Distinguishing between two types of ground velocity is important in the forensic analysis of cases of rockbust damage. Utilisation of PGV to describe strainbursting damage may require unreasonable assumptions (anomalous local amplification of ground motion at the tunnel surface). It is more appropriate to try to assess and use bulking velocity, V_{SB}, for that purpose. In case of complex damage (involving both shakedown and strainbursting mechanisms) it is recommended that both types of ground velocities be evaluated.

The forecasting of dynamic demand, which is expected to be imposed on ground support during future mining, also requires a separate treatment of the two aforementioned types of ground velocity. The illustration of this aspect is the main objective of this paper.

Methods for the evaluation of PGV and V_{SB} (including the cases of future mining) have been suggested earlier and presented in a number of publications. In this paper we summarise these methods in a unified methodology which is briefly explained in Section 2. Section 3 demonstrates the results of its application to a real case. The last section discusses the limitations and future work required.

2 Method

A method for assessing peak ground velocities for planned mining steps was proposed by Malovichko (2017). The key components of the method are as follows (Figure 3):

- A catalogue of expected seismicity is produced for the planned mining sequence. In general, any inelastic stress modelling code can be adopted for this. An appropriate clustering algorithm of plastic strain increments (and preferably excavation convergence) makes it possible to convert the modelling results to a seismic catalogue using the expressions for seismic-source parameters presented by Malovichko (2020). The resulting seismic catalogue includes the locations, origin times (mining steps), sizes (expressed in terms of seismic potency) and source mechanisms (moment tensors) of events.
- The modelled seismic catalogue is not used in further analysis on its own. It is combined with the historical observed catalogue relevant for future mining. Deciding which events are relevant is subjective, and it should take the interpretation of past seismicity and future stress conditions into account. For example, a historical large seismic event interpreted as slip along a fault that is expected to remain in similar stress condition for planned mining steps has to be included in the combined seismic catalogue. Alternatively, large recorded events attributed to the volume for which stress conditions have already changed or are expected to change during planned mining (e.g. the volume will be consumed by a cave) need to be excluded from the combined seismic catalogue.
- A size-distribution hazard assessment is conducted (which quantifies the probability of occurrence of a seismic event of a given size within a seismogenic volume and future time interval). A methodology for this analysis is discussed in detail by Mendecki (2016).
- A spatial seismic hazard assessment is conducted (which quantifies the spatial distribution of the probability of occurrence of a seismic event of a given size within a given rock mass volume and future time interval).

- A ground motion prediction equation is established which estimates PGV for a given seismic potency (or moment magnitude) and hypocentral distance. A functional form of the equation suitable for mines is proposed by Mendecki (2019).
- Ground-motion hazard is assessed (which quantifies the probability of exceedance of a given PGV at a given location for a given time interval).

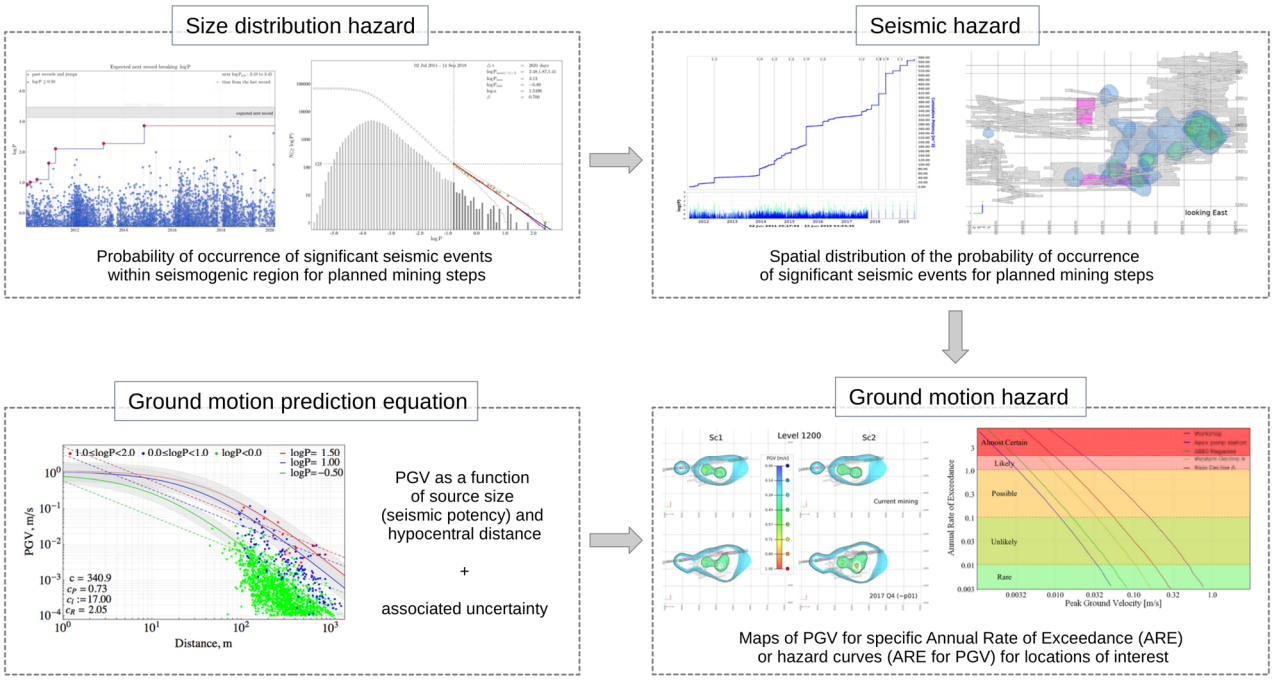

Figure 3 Schematic description of the stages of assessment of peak ground velocity for planned mining steps. The plots shown serve to illustrate the component of the analysis and their details do need to be interpreted

The described method corresponds to the conventional probabilistic seismic hazard assessment (Cornell 1968; McGuire 2004) employed in earthquake engineering. The output of the method is ground motion hazard curves (dependence between PGV and annual rate of exceedance) for locations (e.g. specific tunnels) and future times. The results may also be presented as maps of PGV for a chosen annual rate of exceedance (ARE) which can be selected according to the risk assessment matrix established at the mine. The hazard curves and maps will change over time. Both types of presentation will be illustrated in the next section.

The evaluation of bulking velocity is described by Kaiser & Moss (2022) and Kaiser & Malovichko (2022). The results of evaluation can be presented in probabilistic terms by adopting the framework of fragility functions used in earthquake engineering as discussed by Malovichko (2023). In particular, the assessment of bulking velocities can be accomplished by following these steps (Figure 4):

- Establish the spatial distribution of rock mass properties (specifically UCS) and calculate stresses around the excavations for planned mining steps.
- Calculate the extreme depth of failure, d_f^e, on the perimeter of tunnels using a semi-empirical relation based on the stress level index (Kaiser et al. 1996; Martin et al. 1999; Perras & Diederichs 2016).
- Estimate the bulking duration, t_{SB} , from the duration of P-wave and S-wave pulses of crush-type events associated with tunnels, as described by Malovichko (2023).
- Assess the amount and annual probability of strainbursting realisation (q_{SB} and APE_{SB}) using the approach suggested by Malovichko (2023). The depth of strainbursting is evaluated as $d_{SB} = q_{SB} d_f^e$.

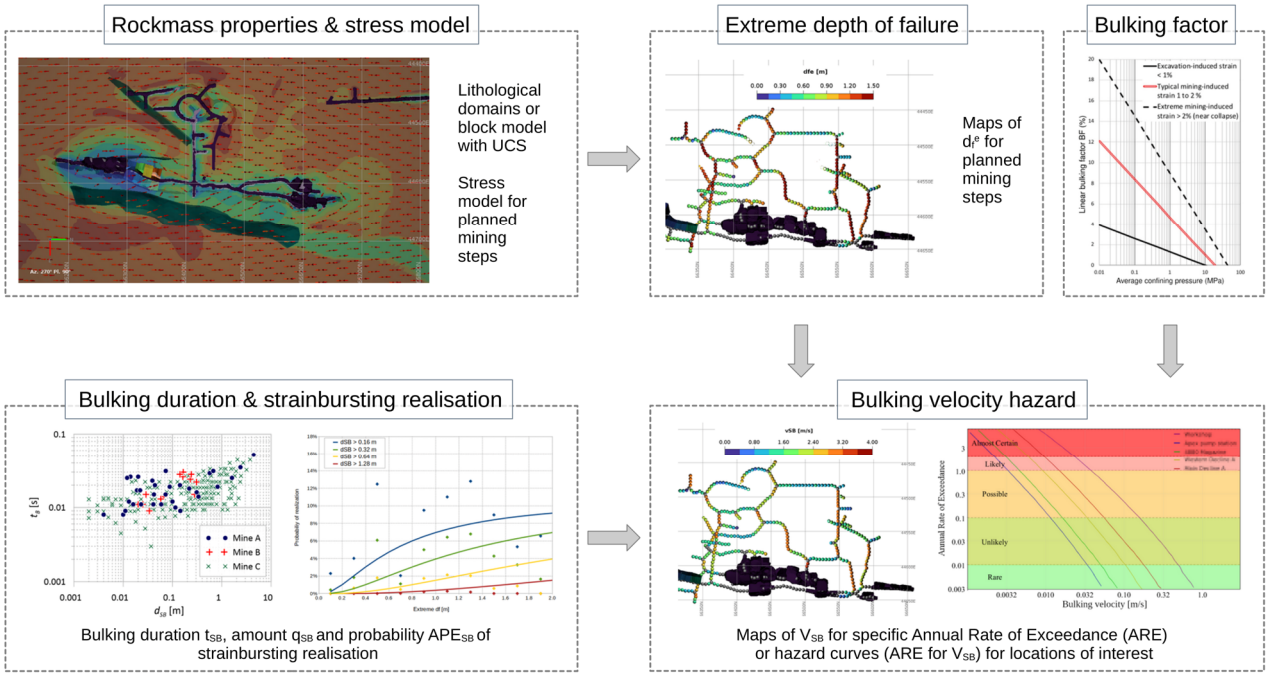

Figure 4 Schematic description of the stages of assessment of bulking velocity for planned mining steps

- Establish an appropriate bulking factor, based on the installed ground support (Kaiser 2016).
- Assess the bulking-velocity hazard (probability of exceedance of given V_{SB} at given tunnel for a given time interval in the future).

The output is the bulking-velocity hazard curve (dependence between V_{SB} and annual rate of exceedance) for locations (e.g. specific tunnels) and future times. The results may also be presented as maps of V_{SB} for a chosen annual rate of exceedance. Both hazard curves and maps depend on time.

3 Application

The assessment of both types of ground velocities for the planned mining sequence is demonstrated using data from a hard rock mine in Australia. The mining layout and stress conditions are presented in Figure 5.

The area under consideration for the analysis is to the side of a sublevel cave. The mining of a sub-horizontal reef extending north–south is conducted using a sequence of primary and secondary stopes. The analysis was conducted in October 2023 for planned mining steps extending to March 2025.

The maximum principal stress is plunging gently southeast. The magnitudes and trajectories of total (in situ and induced) maximum stress assessed using the elastic boundary element model are shown in the top and middle rows of Figure 5.

Mild seismic responses were observed for mining steps up to October 2023. The location and mechanisms of seismic sources indicated that a known structure dipping to the east and located below the reef was activated. The bottom row in Figure 5 shows that the modelling confirms the slip potential of that structure, with further increase of excess shear stress (Ryder 1988) anticipated for future mining steps.

The expected seismic response was modelled using the Salamon–Linkov method (Malovichko & Basson 2014). The parameters of the Mohr–Coulomb failure criteria for the host rock and the seismically active structure were adjusted to match the characteristics of recorded seismicity for the past mining steps (location, size distribution and mechanisms of events). Finally, three scenarios of failure criteria were considered: optimistic, intermediate and pessimistic.

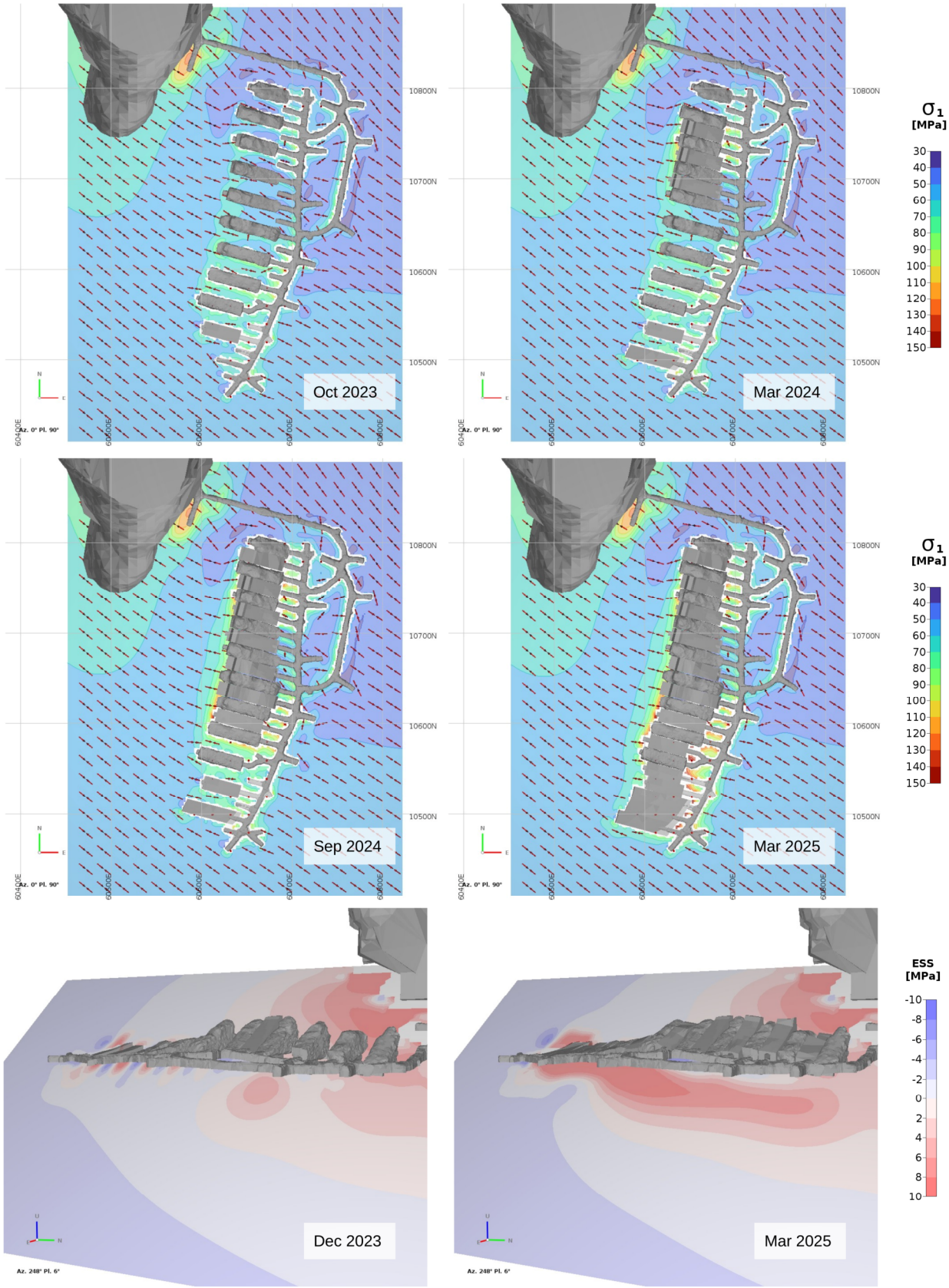

Figure 5 **Mining configuration and stress conditions in the area of analysis. Top and middle: Parameters of the stress field for mining steps. Red dipoles indicate the orientation of maximum principle stress. Bottom: Distribution of excess shear stress for a seismically active structure. A friction angle of 25° was used in the calculations**

The modelled seismic response for planned mining steps for the three scenarios is presented in Figure 6. All of these predict a substantial increase in the rate of potency for future mining steps.

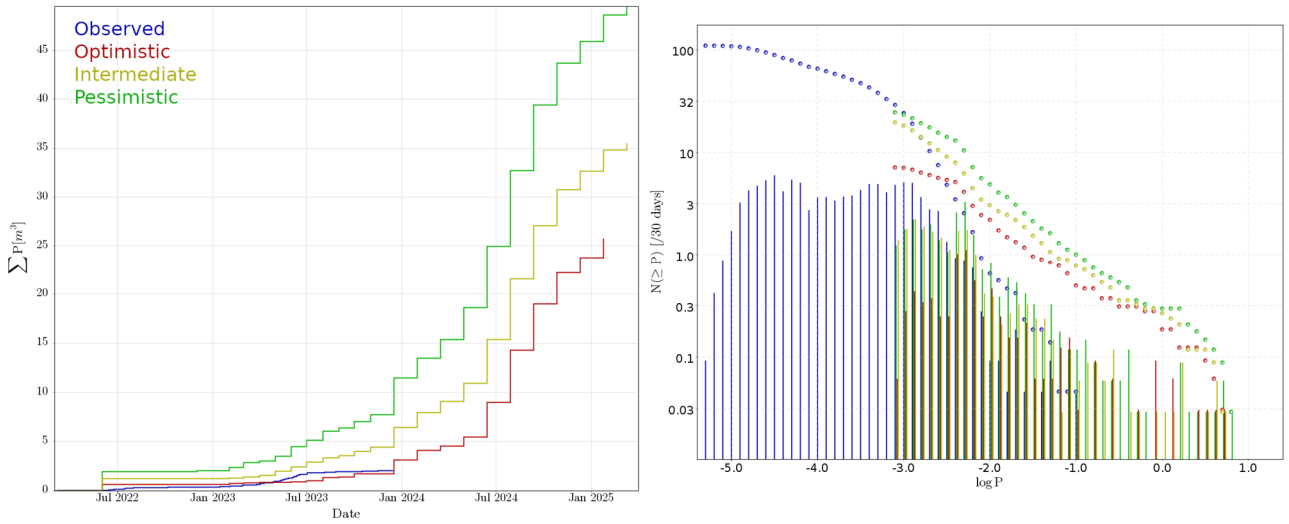

(a) (b)

Figure 6 Time history of cumulative seismic potency (a) and potency–frequency distribution (b) of observed seismicity and modelled seismicity for three scenarios of failure criteria. The number of events in the potency–frequency distribution is normalised to 30 days because the duration of observed and modelled catalogues is different

The spatial distribution of modelled seismicity for the pessimistic scenario combined with the recorded data is shown in Figure 7. A majority of the seismic response is controlled by the geological structure, i.e. many seismic events are located beneath stopes which correspond to episodes of reverse faulting along the structure.

The results of the calculation of peak ground velocities for the pessimistic scenarios of failure criteria are presented in Figures 8 and 9. The velocities increase over time but remain relatively low. The hazard curves for three locations at the entrances of crosscuts indicate that the ground motion exceeding 0.1 m/s corresponds to *unlikely* and *rare* likelihood categories of the risk assessment matrix.

The ARE of 0.01 (boundary of *unlikely* and *rare* likelihood categories) was chosen for plotting the spatial distribution of PGV. The strongest ground motion is expected in the crosscuts during the late stages of mining. The peak ground velocities (for ARE = 0.01) do not exceed 0.4 m/s.

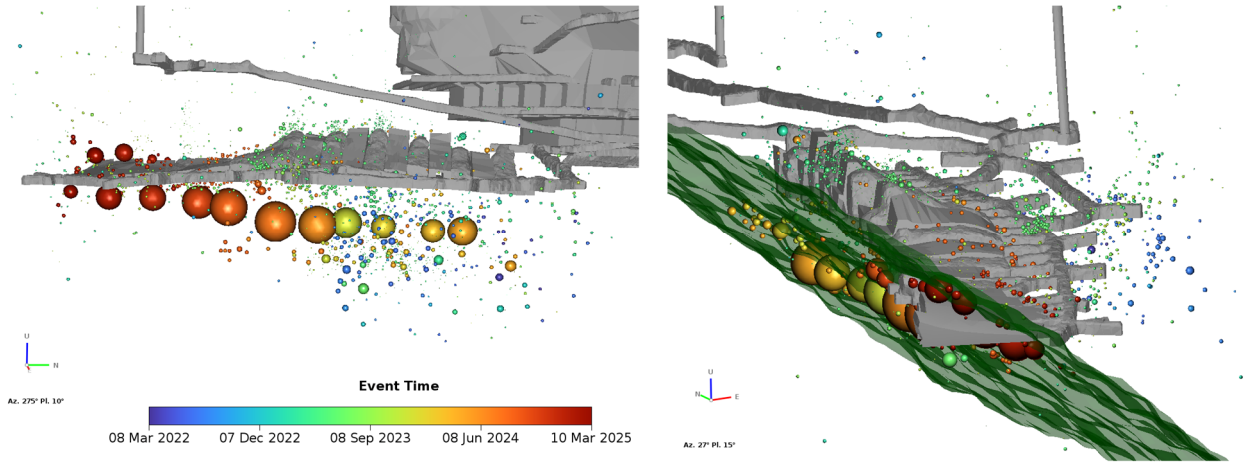

Figure 7 Content of the combined seismic catalogue used for the assessment of peak ground velocities. It includes observed seismicity and modelled seismicity for the pessimistic scenario of failure criteria. The seismically active geological structure is shown in green in the right plot

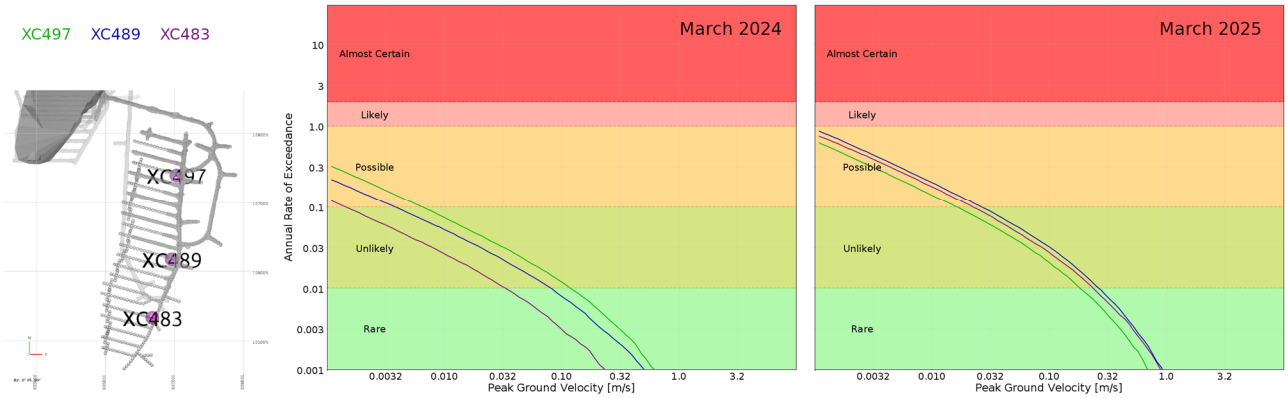

Figure 8 Hazard curves of peak ground velocity for three locations of interest are shown on the left. The horizontal coloured bands correspond to the 'likelihoods' of the risk assessment matrix adopted by the mine

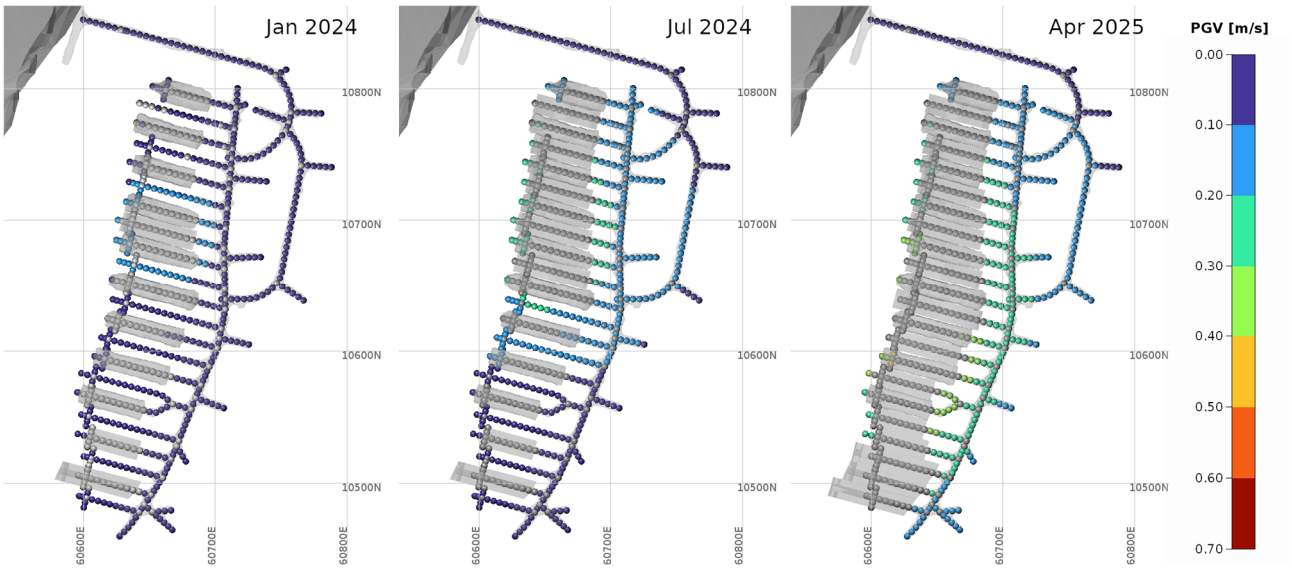

Figure 9 Maps of peak ground velocity for planned mining steps. The presented results correspond to the annual rate of exceedance of 0.01 (boundary of *unlikely* and *rare* categories of the risk assessment matrix). The mined-out stopes are shown using grey wireframes

The results of the calculation of bulking velocities are presented in Figures 10 and 11 in the same format as the peak ground velocities' results. The calculations are based on inelastic stress models (i.e. adopting plastic constitutive relations like Mohr–Coulomb or Hoek–Brown) which include the cave and stopes but exclude tunnels. The maximum tangential stress on the perimeter of tunnels is evaluated using the Kirsch equation. The conducted Monte Carlo simulations take into account the uncertainty of basic input parameters (UCS, BF and t_{SB}), which are defined using triangular distributions. Depths of strainbursting d_{SB} below 0.1 m have been excluded because the utilised bulking durations are not relevant for such small values and these depths are of minor concern regarding the dynamic loading of ground support.

Bulking velocities are somewhat higher than the PGV at the characteristic locations in the crosscuts (Figure 10). The rate of exceedance at low values of V_{SB} is constrained. This is related to the choice of the functional form of strainbursting realisation (Malovichko 2023) and the imposed limitation on d_{SB}.

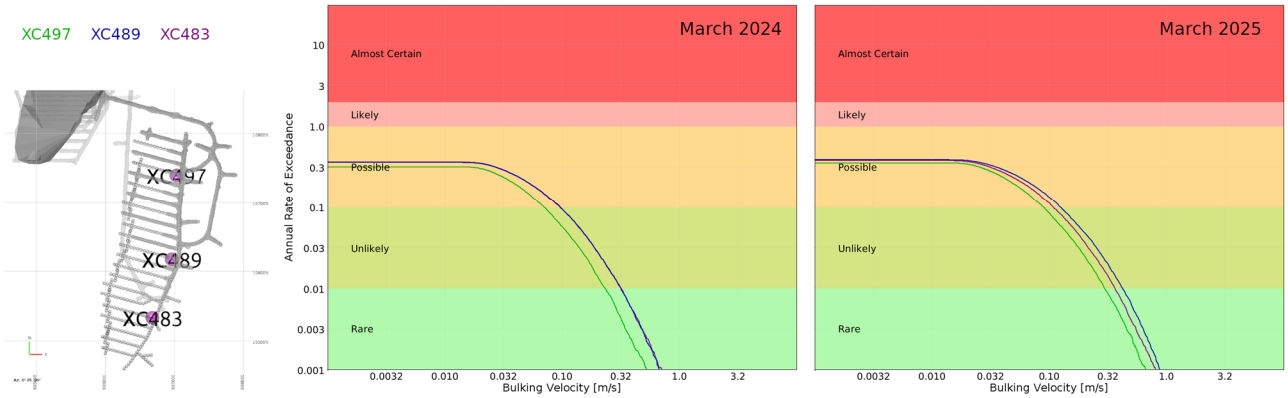

Figure 10 Hazard curves of bulking velocity for three locations of interest

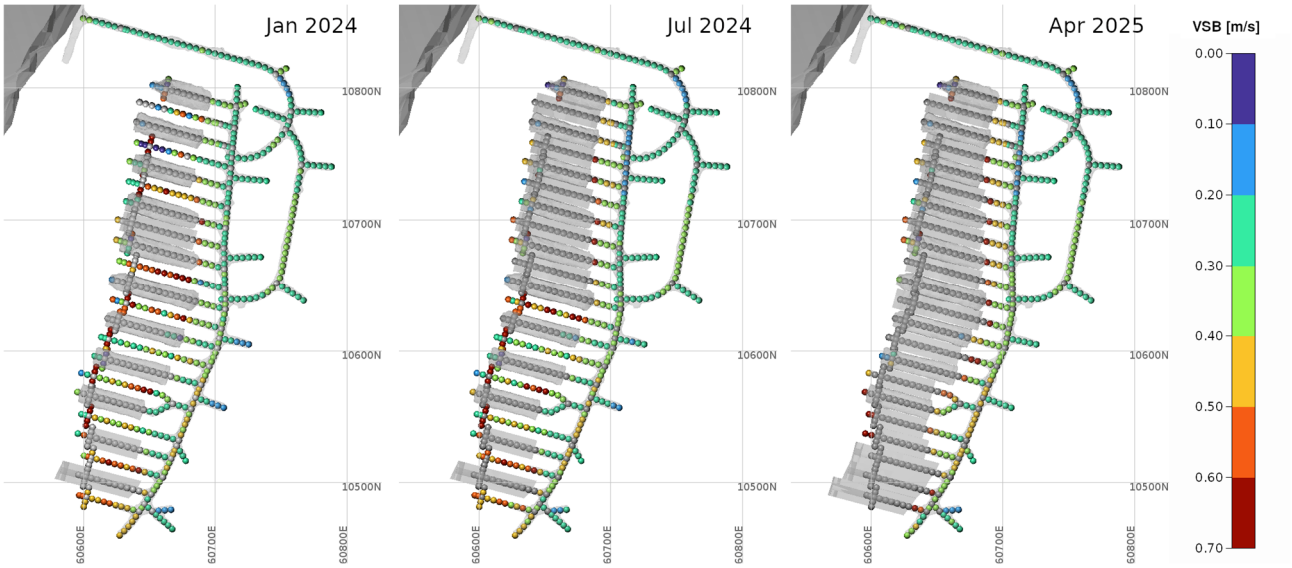

Figure 11 Maps of bulking velocity for planned mining steps. The presented results correspond to the annual rate of exceedance of 0.01 (boundary of *unlikely* and *rare* categories of the risk assessment matrix)

In general, the obtained bulking velocities are larger than the peak ground velocities and therefore the strainbursting hazard is expected to be higher than the shakedown hazard.

The spatial distribution of V_{SB} for ARE = 0.01 (Figure 11) has a different pattern compared to PGV: higher velocities are expected in the stope abutments. Also note that the tunnels oriented in a north–south or northeast–southwest direction in general have higher V_{SB}, than the tunnels having orthogonal directions. This corresponds to differences in the amplitude of maximum tangential stress.

4 Conclusion and discussion

This paper serves to illustrate the importance of the separate assessment of two types of ground velocities: peak ground velocity, which is relevant for the evaluation of shakedown damage likelihood; and the velocity of bulking, required for the evaluation of strainburst likelihood. Methods for the probabilistic assessment of both velocities have been briefly described and demonstrated through their application to a real case (a planned mining sequence in a hard rock mine).

Various direct measurements can potentially improve the reliability of forecasting of ground velocities:

- The presented assessment of peak ground velocities does not take the local amplification of ground motion on the skin of excavations into account. The amplification can be measured (Cuello et al. 2017) and a corresponding adjustment can be applied to the forecast PGV. This may not play an important role as the amplification is typically attributed to ground velocities at high frequencies (i.e. above 100 Hz), and the resulting relative displacement between the host rock and supported/reinforced ground will not be magnified (Malovichko & Kaiser 2020).
- The duration of bulking/strainbursting, t_{SB}, is currently evaluated from seismic data using the method described by Malovichko (2023). The method relies on a number of assumptions about the spatio-temporal characteristics of dynamic stress fracturing around a tunnel. The high-sampling measurements using the load cells installed at rockbolts in strainbursting ground can provide direct assessment of bulking duration. An example of such observations is given by Moraga et al. (2023).
- Bulking factor, BF, is a critical ingredient in the calculation of V_{SB}, and it is not constrained by seismic data. The measurements done by extensometers are important for validating the selected values of BF.
- The evaluation of depth of strainbursting, d_{SB}, is an intermediate step in the forecasting of V_{SB}. The calculated d_{SB} can be verified by observations in test holes.
- The forecast surface displacement of bursting ground, $u_{SB} = BF \cdot d_{SB}$, can also be verified by convergence measurements and laser scans.

Acknowledgement

The permission of the mine to present real data is highly appreciated. We thank the reviewers for their constructive and helpful comments.

References

Cornell, C 1968, 'Engineering seismic risk analysis', *Bulletin of the Seismological Society of America*, vol. 58, pp. 1583–1606.

Cuello, D, Mendecki, A & Mountfort P 2013, 'Ground motion amplification at the skinof excavations, in J Vallejos (ed), *Proceedings of the 9th International Symposium on Rockbursts and Seismicity in Mines*, pp. 216–220.

Kaiser, P 2016, 'Ground support for constructability of deep underground excavations - challenges of managing highly stressed ground in civil and mining projects', *Sir Muir Wood lecture of International Tunnelling Association at World Tunnelling Congress*, p. 33.

Kaiser, P & Moss, A 2022, 'Deformation-based support design for highly stressed ground with a focus on rockburst damage mitigation', *Journal of Rock Mechanics and Geotechnical Engineering,* vol. 14, issue 1, pp. 50–66.

Kaiser, PK & Malovichko, DA 2022, 'Energy and displacement demands imposed on rock support by strainburst damage mechanisms', in M Diederichs (ed), *Proceedings of the 10th International Symposium on Rockbursts and Seismicity in Mines*, Society for Mining, Metallurgy & Exploration, Englewood.

Kaiser, PK, McCreath, D & Tannant, D 1996, *Canadian Rockburst Support Handbook*, Geomechanics Research Center, Sudbury.

Malovichko, DA 2017, 'Assessment and testing of seismic hazard for planned mining sequences', in J Wesseloo (ed.), *Deep Mining 2017: Proceedings of the Eighth International Conference on Deep and High Stress Mining*, Australian Centre for Geomechanics, Perth, pp. 61–77, https://doi.org/10.36487/ACG_rep/1704_02_Malovichko

Malovichko, D 2020, 'Description of seismic sources in underground mines: theory', *Bulletin of the Seismological Society of America*, vol. 110, pp. 2124–2137.

Malovichko, D 2023, 'Utilisation of seismic data in the assessment of displacement and energy demand imposed on ground support by strainbursts', in J Wesseloo (ed.), *Ground Support 2023: Proceedings of the 10th International Conference on Ground Support in Mining*, Australian Centre for Geomechanics, Perth, pp. 181–196, https://doi.org/10.36487/ACG_repo/2325_12

Malovichko, D & Basson, G 2014, 'Simulation of mining-induced seismicity using the Salamon–Linkov method', in M Hudyma & Y Potvin (eds), *Deep Mining 2014: Proceedings of the Seventh International Conference on Deep and High Stress Mining*, Australian Centre for Geomechanics, Perth, pp. 667–680, https://doi.org/10.36487/ACG_rep/1410_47_Malovichko

Malovichko, D & Kaiser, PK 2020, 'Dynamic model for seismic shakedown analysis', *Proceedings of the 54th US Rock Mechanics/Geomechanics Symposium*, ARMA 20-A1461.

Martin, CD, Kaiser, PK & McCreath, DR 1999, 'Hoek-Brown parameters for predicting the depth of brittle failure around tunnels', *Canadian Geotechnical Journal*, vol. 36, no. 1, pp. 136–151.

McGuire, R 2004, *Seismic Hazard and Risk Analysis*, MNO-10, EERI.

Mendecki, AJ 2016, *Mine Seismology Reference Book: Seismic Hazard*, http://www.imseismology.org/msrb/

Mendecki, AJ 2019, 'Simple GMPE for underground mines', *Acta Geophysica*, vol. 67, pp. 837–847.

Moraga, CV, Bahamondes CB, Pulgar, DV & Romero, DC 2023, 'Instrumentación geotécnica para túneles con sismicidad inducida', *Primer Congreso Chileno | Mecánica de Rocas*.

Perras, MA & Diederichs, MS 2016, 'Predicting excavation damage zone depths in brittle rocks', *Journal of Rock Mechanics and Geotechnical Engineering*, vol. 8, no. 1, pp. 60–74.

Rigby, A, Malovichko, D & Kaiser, PK 2024, 'Simulating the displacement and energy demand imposed by a strainburst near a tunnel, in P Andrieux & D Cumming-Potvin (eds), *Deep Mining 2024: Proceedings of the 10th International Conference on Deep and High Stress Mining*, Australian Centre for Geomechanics, Perth, pp. 1399–1414.

Ryder, JA 1988, 'Excess shear stress in the assessment of geologically hazardous situations', *Journal of the Southern African Institute of Mining and Metallurgy*, vol. 88, no. 1, pp. 27–39.